Hydrostatic pressure stabilizes HIF-1α expression in cancer cells to protect against oxidative damage during metastasis

DA ZHAI[1,2], YONG XU[1,2], LINA ABDELGHANY[1,2,3], XU ZHANG[1,2], JINGYAN LIANG[4], SHOUHUA ZHANG[5], CHANGYING GUO[6] and TAO-SHENG LI[1,2]

[1]Department of Stem Cell Biology, Atomic Bomb Disease Institute, Nagasaki University; [2]Department of Stem Cell Biology, Nagasaki University Graduate School of Biomedical Sciences, Nagasaki 852-8523, Japan; [3]Department of Pharmacology and Toxicology, Faculty of Pharmacy, Tanta University, Tanta 31527, Egypt; [4]Institute of Translational Medicine, Medical College, Yangzhou University, Yangzhou, Jiangsu 225000; [5]Department of General Surgery, Jiangxi Provincial Children's Hospital; [6]Department of Thoracic Surgery, Jiangxi Cancer Hospital, Nanchang, Jiangxi 330000, P.R. China

Received November 6, 2020; Accepted April 23, 2021

DOI: 10.3892/or.2021.8162

Abstract. The tissue microenvironment is known to play a pivotal role in cancer metastasis. Interstitial fluid hydrostatic pressure generally increases along with the rapid growth of malignant tumors. The aim of the present study was to investigate the role and relevant mechanism of elevated hydrostatic pressure in promoting the metastasis of cancer cells. Using a commercial device, Lewis lung cancer (LLC) cells were exposed to 50 mmHg hydrostatic pressure (HP) for 24 h. The survival time and morphology of the cells did not notably change; however, the results from a PCR array revealed the upregulation of numerous metastasis-promoting genes (*Hgf*, *Cdh11* and *Ephb2*) and the downregulation of metastasis suppressing genes (*Kiss1*, *Syk* and *Htatip2*). In addition, compared with that in the control, the cells which had undergone exposure to 50 mmHg HP showed significantly higher protein expression level of HIF-1α and the antioxidant enzymes, SOD1 and SOD2, as well as improved tolerance to oxidative stress ($P<0.05$ vs. control). Following an intravenous injection of the LLC cells into healthy mice, to induce lung metastasis, it was found that the exposure of the LLC cells to 50 mmHg HP for 24 h, prior to injection into the mice, resulted in higher cell survival/retention in the lungs 24 h later and also resulted in more metastatic tumor lesions 4 weeks later ($P<0.05$ vs. control). Further investigation is required to confirm the molecular mechanism; however, the results from the present study suggested that elevated interstitial fluid HP in malignant tumors may promote the metastasis of cancer cells by stabilizing HIF-1α expression to defend against oxidative damage.

Correspondence to: Professor Tao-Sheng Li, Department of Stem Cell Biology, Atomic Bomb Disease Institute, Nagasaki University, 1-12-4 Sakamoto, Nagasaki 852-8523, Japan
E-mail: litaoshe@nagasaki-u.ac.jp

Key words: hydrostatic pressure, HIF-1α, metastasis, oxidative stress, adhesion

Introduction

Metastasis occurs in ~90% of malignant tumors and is the leading cause of cancer-associated mortality in patients with cancer worldwide (1,2). A number of biological factors and multiple signaling pathways, such as epithelial-mesenchymal transition, resistance to apoptosis and angiogenesis have been associated with the complex processes of metastasis (3); however, a novel approach for effectively controlling tumor metastasis is still required.

Metastasis is defined as cancer cells leaving the original tumor mass and disseminating to other parts of the body via the bloodstream or lymphatic system. Therefore, the metastatic process represents a multi-step event (3). For example, remote hematogenous metastasis requires the cancer cells to successfully pass through the following steps: i) Transendothelial migration into the vessel (known as intravasation); ii) survival in the circulatory system; iii) attachment to the vessel wall and transendothelial migration out of the vessel (known as extravasation) and iv) eventually live and propagate at the distal site (4,5). All of these steps are accompanied with a change in the surrounding microenvironment, with various biomechanical forces and oxidative stress (6); therefore, metastasis can be a stressful and inefficient event to the cancer cell (7).

Biomechanical forces have been demonstrated to play critical roles in regulating cell migration and proliferation (8,9). With the rapid advancement of mechanobiology in recent years, it has become a hot topic for understanding how biomechanical forces mediate malignant tumor progression (2,8). Beyond the mechanical stress during metastatic processes, it is also well-known that elevated interstitial fluid hydrostatic pressure (HP) occurs in solid tumors (10,11). Higher interstitial fluid HP in tumor mass has been demonstrated to be associated with a worse prognosis in patients with head and neck cancer (12). Furthermore, the exposure of cancer cells to 20 mmHg HP has been demonstrated to accelerate cell motility (8). However, it is not clear whether and how the elevation of interstitial fluid HP in tumor mass promotes the metastasis of cancer cells.

Notably, it has recently been reported that cyclical mechanical force can induce the stabilization of HIF-1α and upregulate the protein expression level of CXCL2 in monocytes (13). HIF-1α is well-known as a master upstream regulator of oxidative stress, metabolism and DNA repair of cells (14-16). Therefore, we hypothesized that elevated interstitial fluid HP in a rapid growing malignant tumor may stabilize HIF-1α to promote the metastasis of cancer cells.

In the present study, mouse Lewis lung carcinoma (LLC) cells were exposed to 50 mmHg HP for 24 h, then the role of HP on the metastatic property of these cells was investigated using both *in vitro* and *in vivo* experiments.

Materials and methods

Cells and animals. The LLC cells (LL/2) were used for the experiments. The cells were maintained in DMEM (FUJIFILM Wako Pure Chemical Corporation), supplemented with 10% fetal bovine serum (Cytiva) and 1% penicillin/streptomycin (Gibco; Thermo Fisher Scientific, Inc.), and cultured at 37˚C in a humidified incubator with 5% CO_2.

A total of 19, male C57BL/6 mice (10-12 weeks old; weight, 23-25 g; CLEA Japan, Inc.) were used for the *in vivo* study. The mice were kept in specific, pathogen-free conditions and were allowed free access to food and water under a controlled temperature (24±1˚C) with 55% humidity in a 12-h light/dark cycle. The animal experiments were approved by the Institutional Animal Care and Use Committee of Nagasaki University (approval no. 1608251335-11). All the animal procedures were performed in accordance with institutional and national guidelines. At the end of the experiments, the mice were administered with general anesthesia using an intraperitoneal injection of mixed anesthetics (0.75 mg/kg medetomidine, 4 mg/kg midazolam and 5 mg/kg butorphanol) and sacrificed by severing the abdominal aorta for blood removal. The removal of vital organs (lung tissue) was used as confirmation of the death of the mice following sacrifice.

HP stimulation. *HP* was induced in the LLC cells using a pneumatic pressurizing system (Strex. Inc.). Briefly, the LLC cells were seeded in 60 mm diameter Petri dishes ($1x10^5$ cells/dish) and cultured for 36 h to form an adherent monolayer. The culture dishes were then randomly selected to move into a sealed chamber in which 50 mmHg HP was stably applied using the pneumatic pressurizing system and kept for 24 h (HP group). The culture dishes without HP exposure were used as the control (CON group).

Cell morphology observation and cell count. Cell morphology was observed under a light microscope (1X71S8F-3; Olympus Corporation) at x200 magnification, 24 h following HP exposure. Then, the cells were collected as a single cell suspension to measure the total cell number using a TC20™ Automated Cell Counter (Bio-Rad Laboratories, Inc.).

Reverse transcription (RT)^2 Profiler™ PCR array. To investigate the mRNA expression level of genes associated with metastasis, RNA was isolated from the cells using a Quick-RNA™ MicroPrep kit (Zymo Research Corp.). The concentration of RNA was measured using a NanoDrop® 2000 spectrophotometer (Thermo Fisher Scientific, Inc.). Then, 1 μg RNA was used to generate cDNA using the RT^2 First Strand kit (Qiagen Corporation), at 25˚C for 10 min, 42˚C for 60 min, then 85˚V for 5 min. Mouse Tumor Metastasis RT^2 Profiler™ PCR array (cat. no. 330231; Qiagen Corporation) was used with a RT^2 SYBR-Green Master mix, according to the manufacturer's instructions and a Roche LightCycler 480 machine (Roche Diagnostics). The array contained a total of 84 genes associated with metastasis. The genes included in the assay were also defined by biological function by the manufacturer. The fold change in expression to the control was calculated using a web-based data analysis program (https://geneglobe.qiagen.com/jp/analyze). Among the 5 available housekeeping genes (*Actb, B2m, Gapdh, Gusb* and *Hsp90ab1*) in the array, *Actb*, *Gusb* and *Hsp90ab1* were automatically selected as the optimal set of internal control for normalization.

Adhesion assay. To evaluate the adhesion ability, the cells from both the HP and CON groups were harvested as single cell suspensions. Freshly harvested cells ($5x10^4$ cells in 5 ml DMEM) were seeded onto a 25-cm^2 Collagen I-coated Flask (Thermo Fisher Scientific, Inc.). Following incubation for 60 min, the unattached cells were gently removed by washing with PBS twice. The number of adherent cells was counted under a light microscope at x200 magnification. The average cell count from >20 randomly selected fields was used for statistical analysis.

Western blot analysis. The protein expression level of HIF-1α, SOD1 and SOD2 was evaluated using western blot analysis, as previously described (17). Total protein from the cells was extracted using 1X RIPA buffer (FUJIFILM Wako Pure Chemical Corporation) and the concentration was detected using a BCA assay. A total of 30 μg protein from each sample was separated using 10-12% SDS-PAGE, then transferred to 0.2-μm PVDF membranes (Bio-Rad Laboratories, Inc.). After blocking with 5% skimmed milk for 1 h at room temperature, the membranes were incubated with primary antibodies against HIF-1α (1:250 dilution; cat. no. ab1; room temperature for 2 h; Abcam), SOD1 (1:500 dilution; cat. no. sc11407; overnight at 4˚C; Santa Cruz Biotechnology, Inc.), SOD2 (1:500 dilution; cat. no. sc30080; overnight at 4˚C; Santa Cruz Biotechnology, Inc.) and β-actin (1:1,000 dilution; cat. no. 8457S; overnight at 4˚C; Cell Signaling Technology, Inc.), followed by incubation with horseradish peroxidase-conjugated secondary antibodies (rabbit anti-mouse, 1:1,000 dilution; cat. no. P026002; goat anti-rabbit, 1:1,000 dilution; cat. no. P044801) (both from Dako; Agilent Technologies, Inc.) at room temperature for 1 h. The expression level was visualized using an enhanced chemiluminescence detection kit (Thermo Fisher Scientific, Inc.). Semi-quantitative analysis was done using ImageQuant LAS 4000 mini detection system (v1.0; GE Healthcare Life Sciences).

Evaluation of oxidative stress tolerance. To evaluate oxidative stress tolerance, the cells from both groups were treated with 0, 20 or 50 μM hydrogen peroxide (H_2O_2) in PBS at 37˚C for 2 h. The apoptotic cells were stained with Annexin V-FITC, while the necrotic cells were labelled with PI using an

Annexin V-FITC Apoptosis Detection Kit (Abcam). The cells without staining were used as negative control. Quantitative flow cytometry analysis was performed using a FACSVerse™ flow cytometer and analyzed using BD FACSuite Software (v1.2 Suite 1.0.2) (both from BD Biosciences).

In addition, intracellular reactive oxygen species (ROS) was detected in the cells. Briefly, the cells from both groups were treated with 0, 20 or 50 μM H_2O_2 in PBS at 37˚C for 1 h, then incubated with 10 μM general oxidative stress indicator (CM-H2DCFDA; Invitrogen; Thermo Fisher Scientific, Inc.) for another 30 min in the dark. Cells without staining were used as a negative control. The accumulation of intracellular ROS was measured by fluorescence intensity using a FACSVerse™ flow cytometer (BD Biosciences) and analyzed using BD FACSuite Software (v1.2 Suite 1.0.2) (both from BD Biosciences).

Experimental lung cancer metastasis model. To evaluate the metastatic potency, experimental lung cancer metastasis was induced in mice using an intravenous injection of LLC cells ($5x10^5$ cells in 0.5 ml saline) from the HP (n=6) and the CON (n=7) groups. A total of 4 weeks after the cells were injected into the mice, all the mice were sacrificed as aforementioned. Removal of lung tissue was used for both confirmation of mice death and experimental evaluation. Excised lung tissue was weighed and the number of tumor lesions on the lung surface was counted. For the mice that spontaneously died during the 4-week follow-up period, the date of death was recorded and the lung tissue samples were collected for evaluation. Statistical analysis of the overall survival rate of the mice was also determined.

Immunohistochemical staining. The cell proliferation and microvessel density in the metastatic lesions of the lungs was detected using immunohistochemistry staining. The lungs were fixed in 4% paraformaldehyde for 24 h, at 4˚C, and paraffin-embedded sections (6-μm thick) were deparaffinized and rehydrated (xylene, 2x3 min washes; xylene 1:1 with 100% ethanol, 3 min; 100% ethanol, 2x3 min washes; 95% ethanol, 3 min; 70% ethanol, 3 min; 50% ethanol, 3 min; running cold tap water to rinse). After blocking with 1% BSA in PBS (Sigma-Aldrich; Merck KGaA), the sections were incubated with rabbit anti-mouse Ki67 antibody (cat. no. ab16667; 1:100 dilution;) and rabbit anti-mouse CD31 antibody (cat. no. ab28394; 1:150 dilution) (both from Abcam) overnight at 4˚C, followed by incubation with the Alexa fluorescent 546-conjugated goat anti rabbit IgG(H+L) secondary antibody (cat. no. A11013; 1:350 dilution; Invitrogen; Thermo Fisher Scientific, Inc.) at room temperature for 1 h. Nuclei were stained with 4, 6-diamidino-2-phenylin-dole (DAPI; cat. no. D21490; Thermo Fisher Scientific, Inc.) at room temperature for 5 min. Positive staining was examined under a fluorescent microscope (FV10C-W3; Olympus Corporation). The percentage of Ki67-positive cells was calculated from 10 randomly selected fields of view (5 fields/slide in 2 slides) and used for statistical analysis. The CD31-positive stained structures were counted as microvessels and the average number of microvessels counted from 10 randomly selected fields of view (5 fields/slide in 2 slides) was used for statistical analysis.

PKH26 red fluorescent cell labeling. To evaluate the survival/retention of the LLC cells in the lungs of the mice, the cells were labelled with a PKH26 Red Fluorescent Cell Linker kit (Sigma-Aldrich; Merck KGaA). Briefly, the cells were incubated with 2 μM PKH26 dye for 5 min at room temperature, as the manufacturer's recommendations. Then, the mice were intravenously injected with the PKH26-labelled cells ($1x10^6$ cells in 0.5 ml saline) from the HP (n=3) and the CON (n=3) groups. The mice were sacrificed 24 h following the injection and the lung tissue samples were collected. Cryosections (8-μm thick) of the lung tissues were used for the direct detection of PKH26-labelled LLC cells under a fluorescent microscope (FV10C-W3; Olympus Corporation).

Statistical analysis. The data are presented as the mean ± SD. Statistical significance between two groups was determined using an unpaired t-test (SPSS; v20.0; IBM Corp.). The survival of the mice was analyzed using a Kaplan-Meier curve and statistical significance was determined using the log-rank test (GraphPad Prism; v8.0.1; GraphPad Software, Inc.). $P<0.05$ was used to indicate a statistically significant difference.

Results

Exposure of the LLC cells to 50 mmHg HP altered the mRNA expression level of numerous genes associated with metastasis. Firstly, the mRNA expression level of genes associated with metastasis was analyzed between the HP and CON groups. The RT^2 Profiler™ PCR array revealed that numerous genes were up- or downregulated, with a >1.3-fold difference in the HP group compared with that in the CON group (Table SI). The top 10 up- or downregulated genes are shown in Fig. 1A. Within the top 10 upregulated genes, the upregulation of several adhesion molecules was found, including *Cdh1*, *Cdh11* and *Fn1* (Fig. 1B). In addition, the upregulation of numerous metastasis-promoting genes, such as *Hgf*, *Cdh11* and *Ephb2*, was also found. Within the top 10 downregulated genes, metastasis suppressors, including *Kiss1*, *Syk* and *Htatip2*, were frequently detected (Fig. 1B). The overall change in the gene expression profile indicated the potential role of HP in enhancing metastatic properties of the LLC cells.

HP exposure enhances the adhesion property of the LLC cells. The exposure of the LLC cells to 50 mmHg HP for 24 h did not induce notable morphological changes (Fig. 2A). The total number of harvested cells was also comparable between the groups ($P=0.70$; Fig. 2A), indicating a limited effect of 50 mmHg HP exposure on cell growth.

As the PCR array data indicated the upregulation of numerous adhesion molecules, the adhesion property of the cells was investigated. It was found that the exposure to 50 mmHg HP significantly increased the number of adherent cells on a collagen I-coated flask ($P<0.05$; Fig. 2B).

HP exposure increases the protein expression level of HIF-1α and antioxidant enzymes in the LLC cells. HIF-1α, a master regulator of the cellular adaptive response to hypoxia, is known to play critical roles in metabolic reprogramming (16) and metastasis (14) in cancer cells. Western blot analysis showed

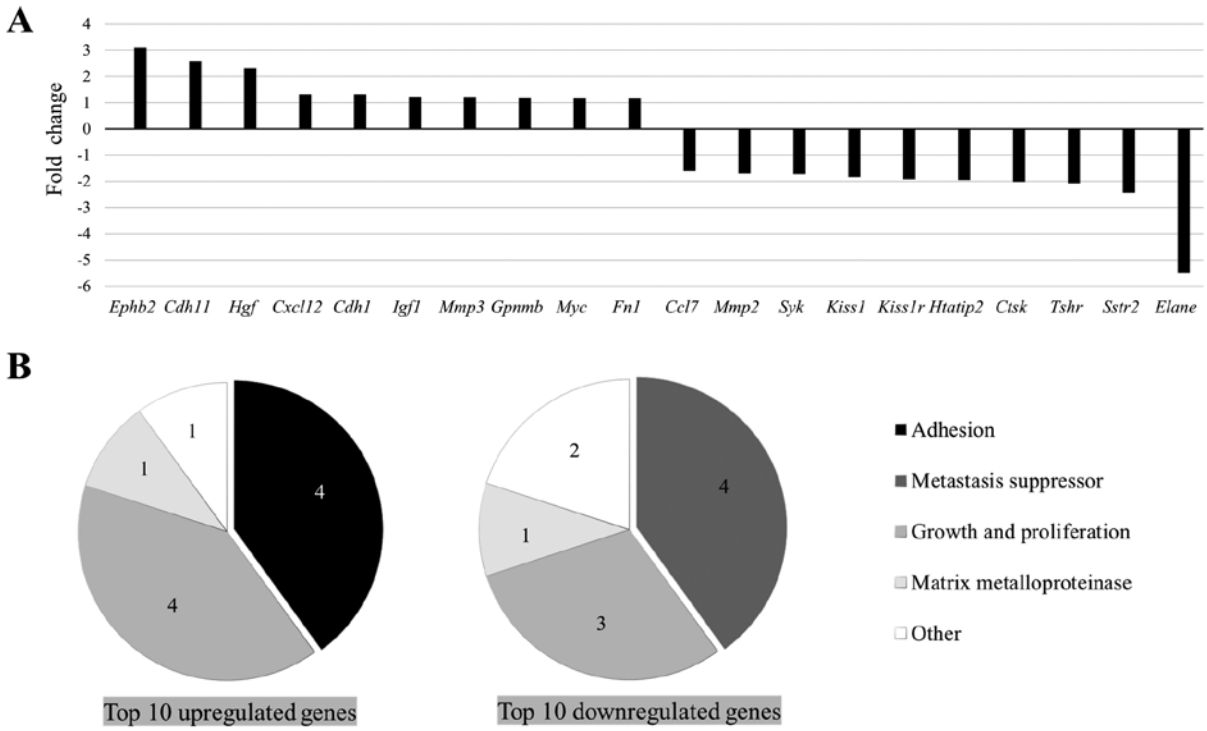

Figure 1. Change in the mRNA expression level of genes in the Lewis lung cancer cells following treatment with or without 50 mmHg HP for 24 h. The mRNA expression level of metastasis-related genes was measured using a reverse transcription^2 Profiler™ PCR array. The data are presented as the fold change in the cells with HP compared with that in the CON. The top 10 up- and downregulated genes are according to the (A) fold change and (B) the biological functional categories of the genes. HP, hydrostatic pressure exposure; CON, control.

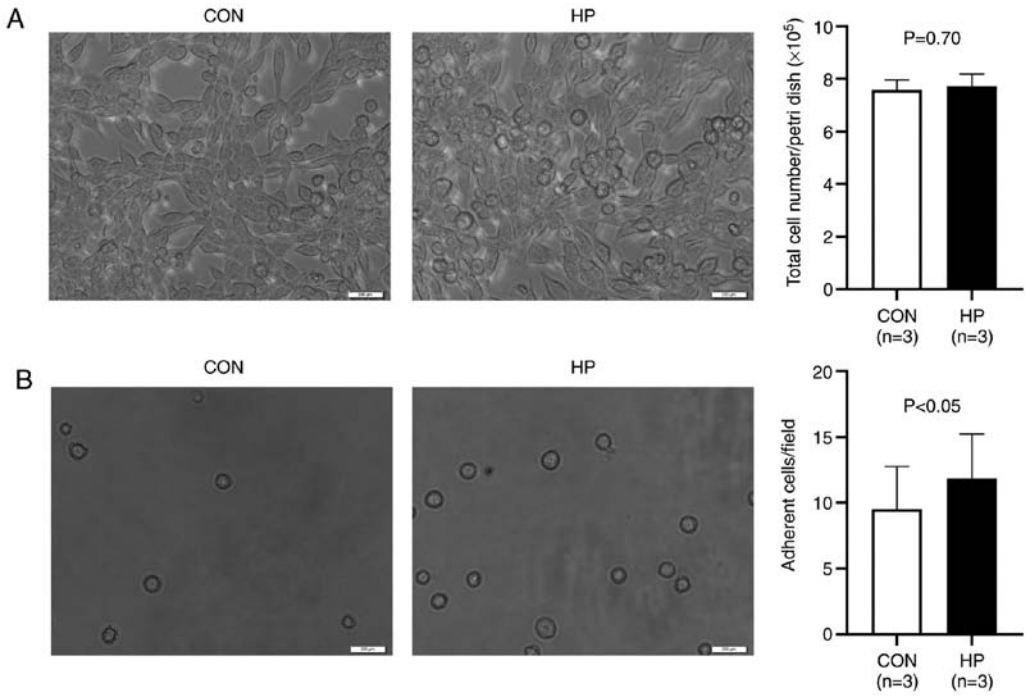

Figure 2. Survival and adhesion property of the Lewis lung cancer cells following treatment with or without 50 mmHg HP for 24 h. (A) Representative images of cell morphology under a phase-contrast microscope (left) and quantitative analysis of the total number of surviving cells per petri dish (right). (B) Representative images (left) and quantitative data (right) of the adherent cells in collagen I-coated flasks. Scale bar, 200 μm. The data are presented as the mean ± SD from 3 independent experiments. HP, hydrostatic pressure exposure; CON, control.

that the protein expression level of HIF-1α was significantly increased in cells exposed to 50 mmHg HP for 24 h (P<0.01; Fig. 3A).

The protein expression level of the antioxidant enzymes, SOD1 and SOD2, which are HIF-1α downstream signals (18,19), was also investigated. As expected, the exposure

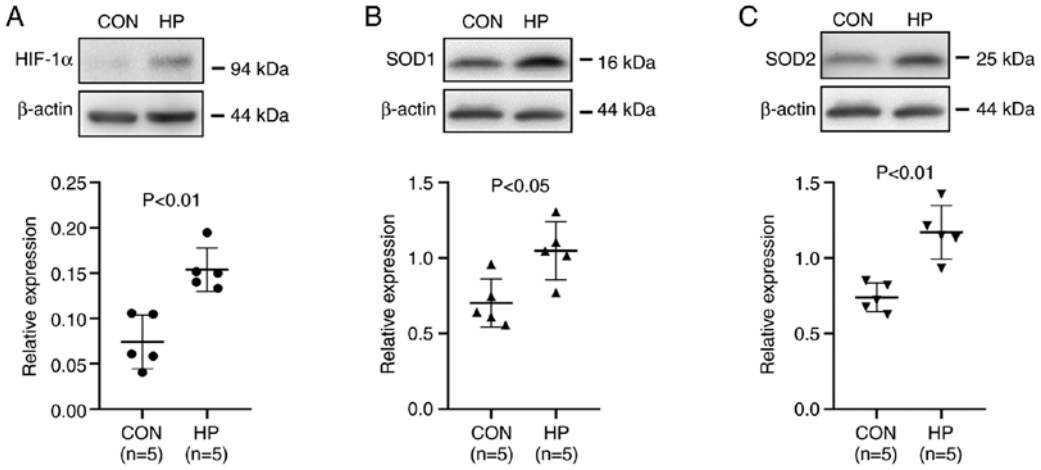

Figure 3. Protein expression level of HIF-1α, SOD1 and SOD2 is increased following exposure of the LLC cells to 50 mmHg HP for 24 h. Representative blots and semi-quantitative analysis of the protein expression level of (A) HIF-1α, (B) SOD1 and (C) SOD2 in the LLC cells following treatment with or without 50 mmHg HP for 24 h. The data are presented as the mean ± SD from 5 independent experiments. HP, hydrostatic pressure; CON, control; LLC, Lewis lung cancer.

of the cells to 50 mmHg HP for 24 h also significantly upregulated the protein expression level of SOD1 and SOD2 (P<0.05; Fig. 3B and C).

HP exposure induces the tolerance of the LLC cells to oxidative stress. In addition, the oxidative stress tolerance of the cells was investigated *in vitro*. Cell necrosis, under 20 or 50 μM H_2O_2 treatment was significantly reduced in the LLC cells pretreated with 50 mmHg for 24 h (P<0.05; Fig. 4A); however, the percentage of apoptotic cells was not significantly different between the 2 groups treated with 20 or 50 μM H_2O_2 (P=0.26 and P=0.45, respectively; Fig. 4A).

The intracellular ROS level at the baseline (without H_2O_2 stimulation) was detected at comparable levels between the HP and CON groups (Fig. 4B). Unexpectedly, 1-h stimulation with 20 or 50 μM H_2O_2 notably decreased the ROS accumulation in the LLC cells without pretreatment with 50 mmHg HP compared with that at baseline (Fig. 4B). By contrast, after 1-h stimulation with 20 μM H_2O_2, the ROS accumulation was slightly increased in the LLC cells pretreated with 50 mmHg HP compared with that at baseline. We hypothesized that the less intracellular ROS accumulation in the LLC cells without HP exposure was due to the severe cell damage or cell death, rather than the resistance to oxidative stress.

HP exposure promotes the metastasis of the LLC cells to the lungs. To evaluate the metastatic potency *in vivo*, the LLC cells were intravenously injected into healthy adult mice. Compared with that in the mice that received LLC cells without HP exposure, significantly worse survival was observed in the mice that received LLC cells pretreated with 50 mmHg HP (P<0.05; Fig. 5A). All the mice were killed 4 weeks following the injection of the cells and the maximum percentage body weight loss observed was 9.3%. There were significantly more metastatic tumor lesions in the lungs of the mice in the HP group compared with that in the CON group (P<0.05; Fig. 5B and C). The weight of the lung tissue was also significantly higher in the HP group compared with that in the CON group (P<0.05; Fig. 5D). These data suggested that HP exposure promoted the metastasis of the LLC cells to the lungs.

To further understand the mechanism involved, the LLC cells were labelled with PKH26 before intravenous injection into the mice, then the survival/retention of the cells in the lungs was analyzed 24 h later. As expected, more LLC cells (or cell clusters) were detected in the lungs from mice in the HP group compared with that in the CON group (Fig. 6A), suggesting an improved survival/retention of the LLC cells by pretreatment with 50 mmHg HP.

Cell proliferation and neovascularization in the metastatic lesions was also analyzed using immunostaining. The percentage of Ki67-positive cells was not significantly different between the HP and CON groups (P=0.20; Fig. 6B). However, the density of the CD31-positive microvessels in the metastatic lesions was significantly higher in the HP group compared with that in the CON group (P<0.05; Fig. 6C).

Discussion

Various mechanical forces within the microenvironment of the tumor mass have been reported to play critical roles in the progression of malignant tumors (2). Owing to the hyper-permeability of immature capillaries, the elevation of the interstitial fluid HP could be commonly induced by the presence of excess fluid accumulation within malignant tumors (20,21). A previous study has reported that HP may drive breast cancer cells toward a more invasive phenotype (9); however, the precise role and relevant mechanism of the mechanical forces in mediating metastasis is still not well understood.

To investigate the role of HP on the metastatic property of cancer cells, the LLC cells were exposed to 50 mmHg HP to mimic the *in vivo* tumor microenvironment, then the mRNA expression level of genes associated with tumor metastasis was analyzed. A PCR array indicated noticeable changes, including the upregulation of metastasis promotors (*Hgf*, *Cdh11* and *Ephb2*) and the downregulation of metastasis suppressors (*Kiss1*, *Syk and Htatip2*) in the LLC cells following exposure to 50 mmHg HP for 24 h. The most upregulated gene, *Ephb2*, has been demonstrated to modulate the metastatic phenotype (22) and induce angiogenesis (23). The most downregulated gene, *Elane*, has been demonstrated to modulate

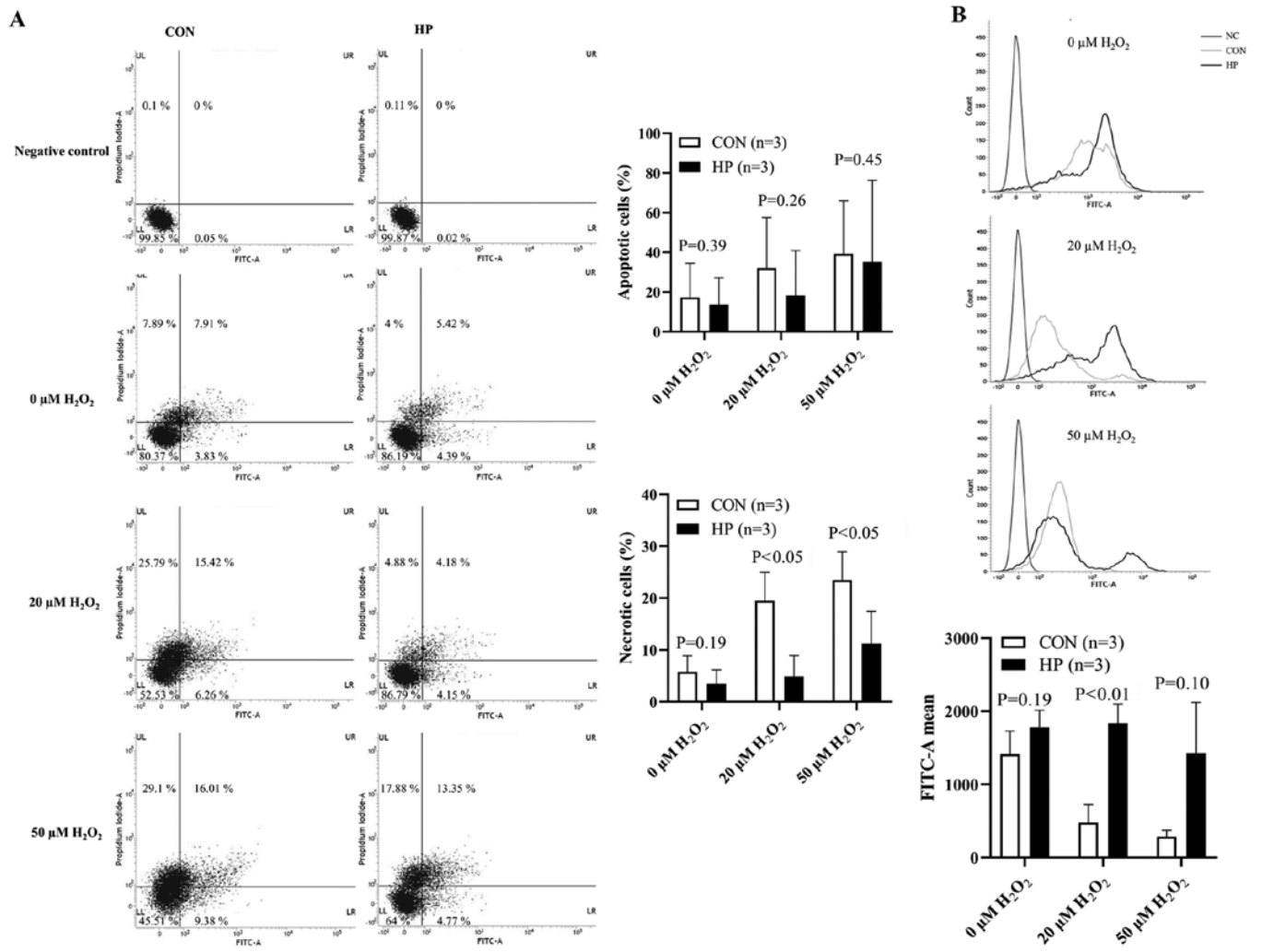

Figure 4. Tolerance of the LLC cells to oxidative stress. The LLC cells were treated with or without 50 mmHg HP and with 0, 20 and 50 μM H_2O_2. The apoptotic/necrotic cells and intracellular ROS was subsequently detected using flow cytometry. (A) Representative flow cytometry plots (left) and quantitative data (right) of the number of apoptotic and necrotic cells. (B) Representative histograms (upper) and quantitative data (lower) of the mean intensity of the intracellular ROS levels. The data are presented as the mean ± SD from three independent experiments. HP, hydrostatic pressure; CON, control; LLC, Lewis lung cancer; ROS, reactive oxygen species; H_2O_2, hydrogen peroxide.

neutrophil expression, inflammation and repair (24). Using an experimental lung metastasis model in mice, it was further confirmed that the LLC cells pretreated with 50 mmHg HP developed a significantly higher number of tumor metastasis lesions in the lungs. These data suggested that an elevated interstitial fluid HP in a rapidly growing malignant tumor may enhance the metastatic property of cancer cells.

Additional experiments were performed to further understand how HP enhanced the metastatic property of the LLC cells from different aspects, according to the multi-step processes of hematogenous metastasis. It is well-known that cancer cells enter the circulation system and are exposed to hyperoxic arterial blood for hematogenous metastasis (6). Accumulating evidence suggests that oxidative stress kills most of the circulating cancer cells, resulting in a very poor efficiency of metastasis (6,7). Therefore, oxidative stress tolerance is essential for the successful metastasis of cancer cells. HIF-1α is well-known as an important mediator of metabolism reprogramming of cancer cells by regulating antioxidant enzymes and antioxidant properties (25). Notably, it has been recently demonstrated that cyclic mechanical force stabilizes HIF-1α by reducing protein degradation (13). Consistently, the results from the present study showed the upregulation of HIF-1α protein expression level in the LLC cells following exposure to 50 mmHg HP for 24 h. In addition, the protein expression level of the antioxidant enzymes, SOD1 and SOD2, the direct downstream targets of HIF-1α (18,19), were also significantly increased in cells exposed to 50 mmHg HP. This could contribute to enhancing antioxidant capacity of cancer cells for remote hematogenous metastasis. Consistent with the upregulation of various adhesion molecules, the exposure to 50 mmHg HP also enhanced the adhesion property of the LLC cells, as shown by the results of the *in vitro* adhesion and the *in vivo* cell tracking assays.

HIFs are heterodimeric proteins composed of HIF-α and HIF-1β subunits. HIF-1α is an O_2-regulated subunit, while HIF-1β is a constitutively expressed subunit (26). The protein expression level of HIF-1α has been reported to be overexpressed in numerous malignant tumors, including lung, prostate, breast and colon carcinomas (27,28). It has been demonstrated that the enhanced protein expression level of HIF-1α was associated with poor prognosis in patients with breast, oropharyngeal and prostate cancer (29-31). As a master regulator of cellular response

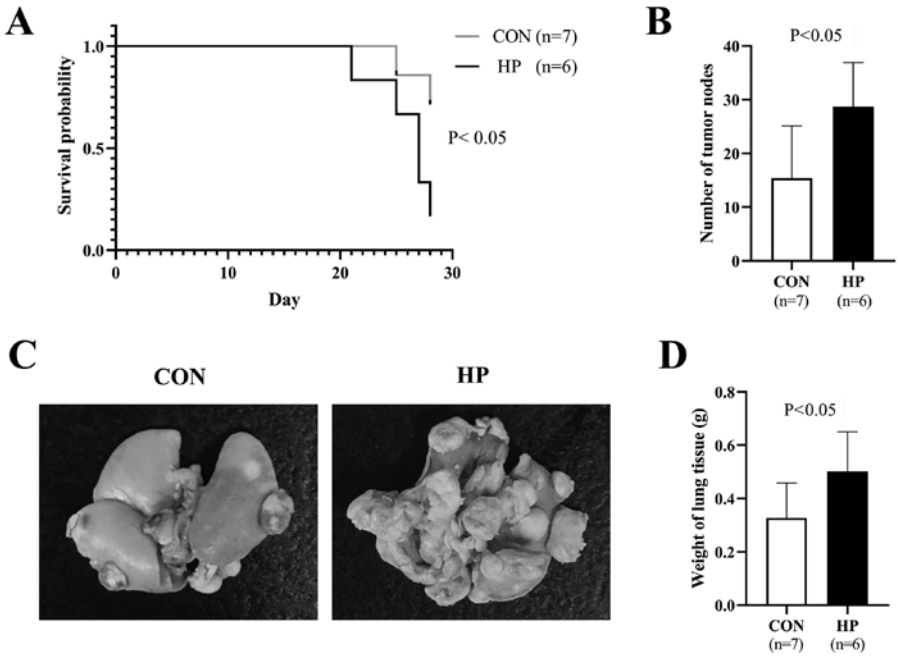

Figure 5. Experimental lung metastasis model in healthy adult mice. The Lewis lung cancer cells were treated with or without 50 mmHg HP and were intravenously injected into the mice, then lung metastasis was evaluated 4 weeks later. (A) Kaplan-Meier curves show the survival probability of the mice. (B) Quantitative data and (C) representative images of tumor metastasis lesions on the surface of lungs. (D) The weight of lung tissues. The data are presented as the mean ± SD. HP, hydrostatic pressure; CON, control.

to hypoxia, HIF-1 can induce the transcription of several genes involved in angiogenesis, cell proliferation and cell metabolism (15,32). One of the most popularly recognized downstream genes of HIF-1 is vascular endothelial growth factor (VEGF), which is known to induce angiogenesis for the rapid growth of malignant tumors (33). VEGF, originally named as vascular permeability factor, was first identified as a tumor-secreted factor, which increases vascular permeability and promotes the accumulation of ascite fluid (21). Considering the hyper-permeability of microvessels in the tumor (34), it is reasonable to hypothesize that an excess accumulation of exudate in the interstitial space contributes, at least in part, to the increase of the interstitial fluid HP in the tumor mass. As a result, elevated HP may stabilize HIF-1α, which thereby induces VEGF and antioxidant enzymes to accelerate the growth and metastasis of malignant tumors.

There is a caution in Cellosaurus that the LLC cells (LL/2) could be identical to 3LL cells. It is reported that LL/2 cell line could be identical to 3LL cell line because both of them are from mouse Lewis lung carcinoma and show the same biological characteristics. Therefore, this will not affect the conclusion of the present study.

A total of 4 weeks after the cells were injected into the mice was used as the humane endpoint, based on clinical signs (reduced intake and activity) and pathophysiological changes (weight loss >20%). During the follow-up for 4 weeks, the progression of tumor metastasis in the lungs of the mice was not directly monitored; however, it was indirectly monitored by observing the clinical signs (intake and activity) and pathophysiological changes (weight loss) of mice.

For the 7 mice that died spontaneously, prior to the end of the 4-week follow-up time in the lung metastasis mice model, it was confirmed that the 7 mice did not die from lung metastasis-induced respiratory failure or systemic cachexia. We hypothesized that the cause of spontaneous death may be due to another cause, based on the following: i) There were no signs of severe clinical symptoms in the 7 mice following daily monitoring; ii) based on the assessment of the exercised lungs, there were fewer metastatic lesions in the lungs of the 7 mice; iii) according to the examination of the 7 mice after sacrifice, there was no serious bleeding, inflammation or purulent secretions in the body, no notable signs of metastasis or organ necrosis was found in the chest cavity or in any of the other organs and no obvious occurrence of cachexia was found.

The present study has several limitations. First, a single cell line was used and the cells were only exposed to 50 mmHg HP for all the experiments. This is due to the following reasons: i) The present study was designed to examine whether an elevated HP could promote the metastasis of cancer cells; ii) the C57BL/6 mice were used for *in vivo* experiments and the LLC cell line is the most reproducible syngeneic model for evaluating lung metastasis to date (35); iii) interstitial fluid pressure in solid malignant tumors could be elevated to ~30 mmHg HP (12,36) and iv) the exposure of the LLC cells to 50 mmHg HP altered the mRNA expression level of genes associated with metastasis; however, higher pressure (100 mmHg) induced cell death and cell debris production (data not shown). Therefore, further experiments are required to exposure different cancer cell lines with different HPs. Second, the PCR array was not repeated due to a limited budget. In addition, the fold-change result may also have greater variations if P>0.05; therefore, it is important to have a sufficient number of biological replicates to validate the array data. However, a mixture of RNA samples was used from three independent experiments to generate the cDNA for a single PCR array in each group. Therefore, the PCR array data was expressed as the average level in 3 samples from each group. Third, further interventional experiments, such as the interference of the HIF-1α signaling

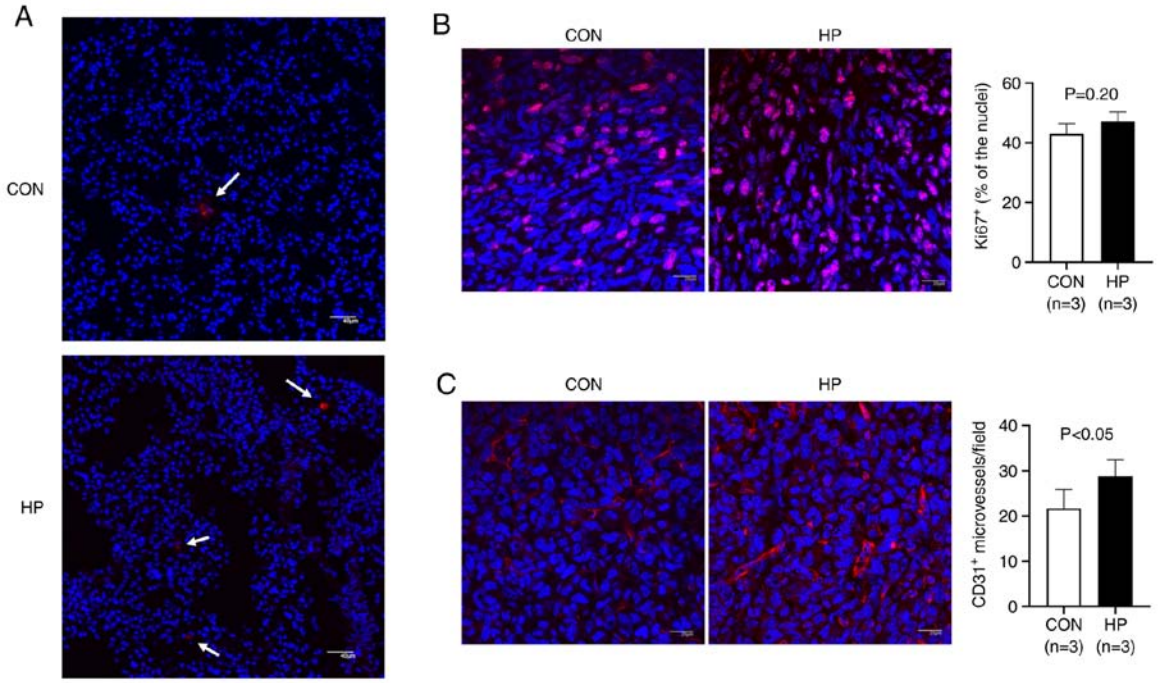

Figure 6. Survival/retention of the LLC cells and immunostaining analysis of proliferating cells and microvessels in the metastatic lesions. The LLC cells were treated with or without 50 mmHg HP, then intravenously injected into the mice. (A) Representative confocal microscopy images of the survival/retention of the PKH26-labelled cells or cell clusters (arrows) in the lungs, 24 h following injection. Scale bar, 40 μm. (B) Representative images (left) and quantitative data (right) of the Ki67-positive proliferative cells in the metastatic lesions in lungs. Scale bar, 20 μm. (C) Representative images (left) and quantitative data (right) of the CD31-positive microvessels in the metastatic lesions in the lungs. Scale bar, 20 μm. The nuclei were stained with DAPI. The data are presented as the mean ± SD. HP, hydrostatic pressure; CON, control; LLC, Lewis lung cancer.

pathway was not performed, as silencing HIF-1α alone would change cell biological properties. Furthermore, multiple factors, including the increase in mRNA expression level of HIF-1α and adhesion molecules could be involved in the HP-induced cancer cell metastasis; therefore, a genetic intervention approach to directly confirm the role of HIF-1α was not performed in the present study. Forth, Annexin V-positive apoptotic cells were only analyzed using flow cytometry and the expression level of other apoptotic proteins, such as the caspase family, can also be used to indicate apoptosis. In addition, a colony-forming assay was not included, as the potential role of HP in cancer cell metastasis, rather than tumorigenesis and tumor growth was the aim of the present study.

From the results in the present study, an elevated HP in rapidly growing malignant tumors may enhance the metastatic potency of cancer cells via complex mechanisms, including the increase in the mRNA expression level of adhesion molecules to improve cell adhesion and the stabilization of HIF-1α to induce the expression of antioxidant enzymes to defend against oxidative damage during metastasis (Fig. 7). It is critical to elucidate the comprehensive molecular mechanisms underlying the stabilization of HIF-1α by HP in further investigations.

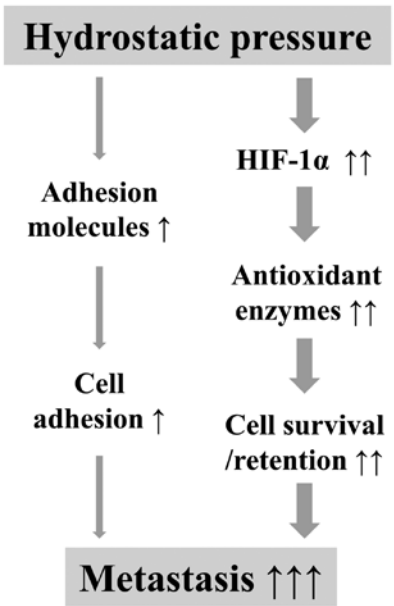

Figure 7. Schematic diagram of hydrostatic pressure induced metastasis of cancer cells. An elevated hydrostatic pressure in malignant tumors may enhance the metastatic potency of cancer cells by i) increasing the mRNA expression level of adhesion molecules to improve cell adhesion, and ii) stabilizing HIF-1α to induce the expression of antioxidant enzymes to protect against oxidative damage.

Acknowledgements

Not applicable.

Funding

This study was supported in part by a Grant-in-Aid from the Ministry of Education, Science, Sports, Culture and Technology, Japan (grant no. 17H04265), the Collaborative Research Program of the Atomic-bomb Disease Institute of Nagasaki University and the Japan China Sasakawa Medical Fellowship.

Availability of data and materials

The datasets used and/or analyzed during the current study are available from the corresponding author on reasonable request.

Author's contributions

All the authors contributed to the conception and design of the study. DZ, YX and LA performed the experiments and acquired the data. TSL, DZ, YX, LA and XZ analyzed and interpreted the data. DZ and SZ drafted the manuscript. TSL, JL and CG critically revised the manuscript for important intellectual content. TSL and DZ confirmed the authenticity of all the raw data. All authors read and approved the final version of the manuscript.

Ethics approval and consent to participate

The animal experiments were approved by the Institutional Animal Care and Use Committee of Nagasaki University (approval no. 1608251335-11) and all animal procedures were performed in accordance with institutional and national guidelines.

Patient consent for publication

Not applicable.

Competing interests

The authors declare that they have no competing interests.

References

1. Brabletz T, Lyden D, Steeg PS and Werb Z: Roadblocks to translational advances on metastasis research. Nat Med 19: 1104-1109, 2013.
2. Bregenzer ME, Horst EN, Mehta P, Novak CM, Repetto T and Mehta G: The role of cancer stem cells and mechanical forces in ovarian cancer metastasis. Cancers 11: 1008, 2019.
3. Eccles SA and Welch DR: Metastasis: Recent discoveries and novel treatment strategies. Lancet 369: 1742-1757, 2007.
4. Fidler IJ: The pathogenesis of cancer metastasis: The 'seed and soil' hypothesis revisited. Nat Rev Cancer 3: 453-458, 2003.
5. Zijl FV, Krupitza G and Mikulits W: Initial steps of metastasis: Cell invasion and endothelial transmigration. Mutat Res 728: 23-34, 2011.
6. Piskounova E, Agathocleous M, Murphy MM, Hu Z, Huddlestun SE, Zhao Z, Leitch AM, Johnson TM, DeBerardinis RJ and Morrison SJ: Oxidative stress inhibits distant metastasis by human melanoma cells. Nature 527: 186-191, 2015.
7. Vanharanta S and Massague J: Origins of metastatic traits. Cancer Cell 24: 410-421, 2013.
8. Kao YC, Jheng JR, Pan HJ, Liao WY, Lee CH and Kuo PL: Elevated hydrostatic pressure enhances the motility and enlarges the size of the lung cancer cells through aquaporin upregulation mediated by caveolin-1 and ERK1/2 signaling. Oncogene 36: 863-874, 2017.
9. Tse JM, Cheng G, Tyrrell JA, Wilcox-Adelman SA, Boucher Y, Jain RK and Munn LL: Mechanical compression drives cancer cells toward invasive phenotype. Proc Natl Acad Sci USA 109: 911-916, 2012.
10. Less JR, Posner MC, Boucher Y, Borochovitz D, Wolmark N and Jain RK: Interstitial hypertension in human breast and colorectal tumors. Cancer Res 52: 6371-6374, 1992.
11. Nathan SS, DiResta GR, Casas-Ganem JE, Hoang BH, Sowers R, Yang R, Huvos AG, Gorlick R and Healey JH: Elevated physiologic tumor pressure promotes proliferation and chemosensitivity in human osteosarcoma. Clin Cancer Res 11: 2389-2397, 2005.
12. Gutmann R, Leunig M, Feyh J, Goetz AE, Messmer K, Kastenbauer E and Jain RK: Interstitial hypertension in head and neck tumors in patients: Correlation with tumor size. Cancer Res 52: 1993-1995, 1992.
13. Solis AG, Bielecki P, Steach HR, Sharma L, Harman CC, Yun S, de Zoete MR, Warnock JN, To SDF, York AG, *et al*: Mechanosensation of cyclical force by PIEZO1 is essential for innate immunity. Nature 573: 69-74, 2019.
14. Rankin EB, Nam JM and Giaccia AJ: Hypoxia: Signaling the metastatic cascade. Trends Cancer 2: 295-304, 2016.
15. Semenza GL: Hypoxia-inducible factors in physiology and medicine. Cell 148: 399-408, 2012.
16. Semenza GL: Regulation of cancer cell metabolism by hypoxia-inducible factor 1. Semin Cancer Biol 19: 12-16, 2009.
17. Urata Y, Goto S, Luo L, Doi H, Kitajima Y, Masuda S, Ono Y and Li TS: Enhanced Nox1 expression and oxidative stress resistance in c-kit-positive hematopoietic stem/progenitor cells. Biochem Biophys Res Commun 454: 376-380, 2014.
18. Hu XQ, Song R and Zhang L: Effect of oxidative stress on the estrogen-NOS-NO-KCa channel pathway in uteroplacental dysfunction: Its implication in pregnancy complications. Oxid Med Cell Longev 2019: 9194269, 2019.
19. Novak S, Drenjancevic I, Vukovic R, Kellermayer Z, Cosic A, Tolusic Levak M, Balogh P, Culo F and Mihalj M: Anti-inflammatory effects of hyperbaric oxygenation during DSS-induced colitis in BALB/c mice include changes in gene expression of HIF-1α, proinflammatory cytokines, and antioxidative enzymes. Mediators Inflamm 2016: 7141430, 2016.
20. Jain RK, Martin JD and Stylianopoulos T: The role of mechanical forces in tumor growth and therapy. Annu Rev Biomed Eng 16: 321-346, 2014.
21. Senger DR, Galli SJ, Dvorak AM, Perruzzi CA, Harvey VS and Dvorak HF: Tumor cells secrete a vascular permeability factor that promotes accumulation of ascites fluid. Science 219: 983-985, 1983.
22. Liu YL, Horning AM, Lieberman B, Kim M, Lin CK, Hung CN, Chou CW, Wang CM, Lin CL, Kirma NB, *et al*: Spatial EGFR dynamics and metastatic phenotypes modulated by upregulated EphB2 and Src pathways in advanced prostate cancer. Cancers (Basel) 11: 1910, 2019.
23. Sato S, Vasaikar S, Eskaros A, Kim Y, Lewis JS, Zhang B, Zijlstra A and Weaver AM: EPHB2 carried on small extracellular vesicles induces tumor angiogenesis via activation of ephrin reverse signaling. JCI Insight 4: e132447, 2019.
24. Makaryan V, Zeidler C, Bolyard AA, Skokowa J, Rodger E, Kelley ML, Boxer LA, Bonilla MA, Newburger PE, Shimamura A, *et al*: The diversity of mutations and clinical outcomes for ELANE-associated neutropenia. Curr Opin Hematol 22: 3-11, 2015.
25. Nakashima R, Goto Y, Koyasu S, Kobayashi M, Morinibu A, Yoshimura M, Hiraoka M, Hammond EM and Harada H: UCHL1-HIF-1 axis-mediated antioxidant property of cancer cells as a therapeutic target for radiosensitization. Sci Rep 7: 6879, 2017.
26. Semenza GL: Pharmacologic targeting of hypoxia-inducible factors. Annu Rev Pharmacol Toxicol 59: 379-403, 2019.
27. Zhong H, De Marzo AM, Laughner E, Lim M, Hilton DA, Zagzag D, Buechler P, Isaacs WB, Semenza GL and Simons JW: Overexpression of hypoxia-inducible factor 1alpha in common human cancers and their metastases. Cancer Res 59: 5830-5835, 1999.
28. Talks KL, Turley H, Gatter KC, Maxwell PH, Pugh CW, Ratcliffe PJ and Harris AL: The expression and distribution of the hypoxia-inducible factors HIF-1alpha and HIF-2alpha in normal human tissues, cancers, and tumor-associated macrophages. Am J Pathol 157: 411-421, 2000.
29. Generali D, Berruti A, Brizzi MP, Campo L, Bonardi S, Wigfield S, Bersiga A, Allevi G, Milani M, Aguggini S, *et al*: Hypoxia-inducible factor-1alpha expression predicts a poor response to primary chemoendocrine therapy and disease-free survival in primary human breast cancer. Clin Cancer Res 12: 4562-4568, 2006.
30. Aebersold DM, Burri P, Beer KT, Laissue J, Djonov V, Greiner RH and Semenza GL: Expression of hypoxia-inducible factor-1alpha: A novel predictive and prognostic parameter in the radiotherapy of oropharyngeal cancer. Cancer Res 61: 2911-2916, 2001.
31. Nanni S, Benvenuti V, Grasselli A, Priolo C, Aiello A, Mattiussi S, Colussi C, Lirangi V, Illi B, D'Eletto M, *et al*: Endothelial NOS, estrogen receptor beta, and HIFs cooperate in the activation of a prognostic transcriptional pattern in aggressive human prostate cancer. J Clin Invest 119: 1093-1108, 2009.

32. Semenza GL: Defining the role of hypoxia-inducible factor 1 in cancer biology and therapeutics. Oncogene 29: 625-634, 2010.
33. Apte RS, Chen DS and Ferrara N: VEGF in signaling and disease: Beyond discovery and development. Cell 176: 1248-1264, 2019.
34. Dvorak HF: Vascular permeability factor/vascular endothelial growth factor: A critical cytokine in tumor angiogenesis and a potential target for diagnosis and therapy. J Clin Oncol 20: 4368-4380, 2002.
35. Kellar A, Egan C and Morris D: Preclinical murine models for lung cancer: Clinical trial applications. Biomed Res Int 2015: 621324, 2015.
36. Mori T, Koga T, Shibata H, Ikeda K, Shiraishi K, Suzuki M and Iyama K: Interstitial fluid pressure correlates clinicopathological factors of lung cancer. Ann Thorac Cardiovasc Surg 21: 201-208, 2015.